SUPPLEMENTAL MATERIAL

Supplemental Methods

Animals

$Kit^{+/Cre\text{-}IRES\text{-}nGFP}$ ($Kit^{+/nGFP}$) mice and $Kit^{+/MerCreMer}$ ($Kit^{+/MCM}$) were previously reported.[1] To perform genetic lineage tracing, mice were cross-bred to either R-GFP (green fluorescent protein) reporter mice (FVB.Cg-*Gt(ROSA)26Sor*$^{tm1(CAG\text{-}lacZ,\text{-}EGFP)Glh}$/J, purchased from the Jackson Laboratory and previously cross-bred with germ line Frt expressing mice to generate GFP reporter mice), or R-mTmG reporter mice (B6.129(Cg)-*Gt(ROSA)26Sor*$^{tm4(ACTB\text{-}tdTomato,\text{-}EGFP)Luo}$/J, purchased from the Jackson Laboratory) and to Super p53 mice (B6;CBA-Tg(Trp53)1Srn/J).[2] All animal procedures were performed in accordance with institutional guidelines, and approved by the University of Minnesota Institutional Animal Care and Use Committee.

Pharmacological treatments

Activation of inducible Cre recombinase was accomplished via either Tamoxifen injection, or Tamoxifen containing chow. Tamoxifen base (Sigma-Aldrich T5648) was dissolved in corn oil and injected intra-peritoneally for 5 consecutive days at 20mg/kg. Tamoxifen citrate containing chow (400mg/kg) was purchased from Harlan/Envigo. Three-month-old mice were treated with tamoxifen-laden chow for four weeks to induce Cre activation to allow genetic lineage tracing of c-kit^+ cells. Tamoxifen-containing chow was replaced with regular chow at least 72hr (6 times elimination half-time) before initiating experiments.[3] $Kit^{+/MCM}$ X R-GFP mice and $Kit^{+/MCM}$ X R-mTmG mice were treated with either one intraperitoneal injection of 5 or 10mg/kg of doxorubicin (DOX, Sigma-Aldrich, Cat #D1515), or two intraperitoneal injections of DOX (10 mg/kg at 3-day intervals, 20 mg/kg cumulative dose). Three-month-old $Kit^{+/nGFP}$ mice were similarly

treated with one or two doses of DOX. Both male and female mice were used for all studies. Littermates that received vehicle (saline) were used as controls. Etoposide (Sigma-Aldrich, E1383) was dissolved in Dimethyl Sulfoxide (DMSO, Sigma-Aldrich, D2650) and was delivered in a similar fashion as DOX. Two intraperitoneal injections of Etoposide (1 mg/kg at 3-day intervals, 2 mg/kg cumulative dose) were administered to $Kit^{+/MCM}$ X R-GFP mice. Control mice received the same volume of DMSO. To block the function of p53, Pifithrin-α (Calbiochem Inc, Cat #506132) was dissolved in DMSO and injections of 4.4 mg/kg were delivered intraperitoneally to the mice 30 min before and 3 hrs after DOX administration, followed by a daily injection at the same dose until the mice were sacrificed. To stabilize p53 protein, the small molecule RITA (Calbiochem Inc, Cat #506149) was dissolved in DMSO and 0.3 mg/kg of RITA was injected intraperitoneally to $Kit^{+/MCM}$ X R-GFP mice twice per week for a total of 4 weeks. Control mice received equal volumes of DMSO.

Mouse surgery

Cardiac pressure overload in mice was induced via transverse aortic constriction (TAC) as described previously.[4] Briefly, 8-12 weeks old $Kit^{+/MCM}$ X R-GFP and $Kit^{+/MCM}$ X R-mTmG mice, that were previously treated with tamoxifen, were anesthetized with inhaled 1.5% isoflurane. A parasternal incision was performed and the lobes of the thymus were separated to expose the transverse aorta. A 27 Gauge blunt needle was ligated against the aorta using 6-0 non-absorbable silk suture. After removal of the needle, the thoracic wall was sutured and the skin was closed using skin glue. Sham operated animals were treated similarly, although the aorta was not ligated. Sham operated animals were used as controls.

Cell isolation

Cardiac CD45$^-$c-kit$^+$ cells were isolated from adult C57Bl/6j mice (the Jackson Laboratory) following a published protocol with minor modifications.[5] Hearts were dissected and digested with Collagenase B, Dispase II (Roche) and DNAse (Amersco) in DMEM media at 37˚C. Following digestion, CD45$^+$ cells were depleted and enriched for c-kit$^+$ cells using magnetic microbeads (Miltenyi). The resulting cells were used for the experiments. Flow cytometry was performed to verify the purity of isolated CD45$^-$c-kit$^+$ cells at every step of the isolation procedure using a BD FACS Aria II (Becton, Dickenson and Company). Cells were stained with CD45-PE, CD117-FITC and a microbead labeling check antibody conjugated to APC (Miltenyi). Propidium iodide (PI) was used as a viability marker. FACS data were analyzed in FlowJo v10. We obtained 95% enrichment of single CD45$^-$c-kit$^+$ cells. For single cell RNA seq we isolated CD45$^-$c-kit$^+$ cells from neonatal or adult C57Bl/6 hearts and from adult Kit$^{+/MCM}$ hearts. Cells were sorted by MACS, followed by PI staining and MoFlo sorting of live cells. Sorted cells were immediately stained for live/dead and used for single cell capture using the Fluidigm C1 capture system on an integrated fluidics circuit optimized for capture of cells sized 5-10μm. This size was based on measurements of CD45$^-$c-kit$^+$ cells from adult mice, which averaged at 8.9μm. After capture, cells were imaged to assess viability, followed by RNA isolation and cDNA generation according to the Fluidigm protocol. Based on acquired images, we selected single live cells to proceed with library preparation, according to the Fluidigm protocol.[6] Libraries were pooled and sequenced on an Illumina HiSeq2500 at the University of Minnesota Genomics Center.

For cell culture experiments, we used neonatal and adult mice to isolate CD45$^-$c-kit$^+$ cells according to the protocol detailed above, and cultured them in media that contained 10ng/mL basic fibroblast growth factor (bFGF), 10ng/mL leukemia inhibitory factor (LIF), and 1% penicillin/streptomycin.[7] 3T3 cells (ATCC) were cultured in DMEM supplemented with 10% FCS and 1% penicillin/streptomycin. C-kit depleted non-

cardiomyocytes were isolated using adult hearts digested with Collagenase B, Dispase II (Roche) and DNAse (Amersco) in DMEM media at 37˚C, followed by depletion of c-kit$^+$ cells using magnetic beads (Miltenyi). Experiments were performed at 70-80% confluency. DOX was added to the medium (0.5 μM final concentration) after which the cells were harvested at different time points (0 hour, 4 hours, and 24 hours after treatment) for either protein extraction or Comet assays.

Adult cardiomyocytes were isolated using retrograde perfusion with Collagenase II in modified Tyrode solution.[1] Immediately after isolation, we enriched for cardiomyocytes by spinning at 10g. An inverted Zeiss Axiovision microscope was used to quantify the fraction of rod shaped cardiomyocytes that was positive for GFP.

Histological analysis

Hearts were harvested and processed for cryostat sectioning by prefixing in 4% paraformaldehyde for 2-3 hrs followed by overnight immersion in 30% sucrose in phosphate buffered saline (PBS). Each heart was cut into 1mm slices along the long axis of the heart using an Adult Mouse Heart Slicer (Zivic Instruments). Each slice was embedded in optimum cutting temperature (OCT, Tissue-Tek) and sectioned at a thickness of 5-10μm. Alternatively, we embedded the harvested hearts in OCT and sectioned through the entire heart. Reporter protein expression was readily observed in the absence of a GFP antibody at high contrast with background levels using either epifluorescence or confocal microscopes. GFP$^+$ cardiomyocytes were quantified using an epifluorescent microscope and a 20x objective. Cardiomyocytes were recognized by their characteristic shape and size. We quantified GFP$^+$ cardiomyocytes on multiple sections from each heart at various sectional planes, typically 6 or more. To represent the GFP$^+$ cardiomyocytes as a percentage, we quantified numbers of cardiomyocytes (c) using Wheat Germ Agglutinin stained sections, and measured the area of

cardiomyocytes (a) from at least 6 separate images. We calculated the average density of cardiomyocytes on these images (d=c/a). Next, we generated a stitched image of an entire heart section and measured the area covered by cardiac muscle (A) using Image J. The total number of cardiomyocytes (T) on a heart section was calculated (T=A*d), and the percentage of GFP^+ cardiomyocytes was derived from this (p=G/T*100%). For immunohistological staining, tissue sections were blocked with blocking buffer, followed by overnight primary antibody incubation at 4˚C. For c-kit immunostaining, freshly isolated hearts were frozen in OCT and sectioned. Sections were blocked with PBS containing 0.5-1% BSA, 2mM EDTA and 0.03% Tween20, followed by overnight incubation with primary antibody at 4˚C. The slides were then rinsed in PBS-T (PBS plus 0.1% Tween-20) three times, and incubated with secondary antibody and DAPI for one hour at room temperature. The slides were rinsed with PBS-T and covered with mounting medium (Vectashield, Cat #H-1000). Images were acquired with a Zeiss Axiovision epifluorescent microscope at the Lillehei Heart Institute or Nikon C2 and A1R confocal microscope at the University of Minnesota – University Imaging Centers, http://uic.umn.edu. The primary antibodies are summarized in the Supplemental Table 1.

Western blotting

For Western blotting, cells were harvested at 0, 4 or 24 hours after addition of saline or DOX. Cells were collected in sample buffer supplemented with protease inhibitors. Proteins were separated using SDS-PAGE and blotted onto nitrocellulose membranes. Membranes were blocked and incubated with primary antibodies against p53 (Cell Signaling Technologies), cleaved caspase 3 (Cell Signaling Technologies) and GAPDH (Fitzgerald Industries Int.). The next day, membranes were washed, incubated with secondary antibodies IRDye 680 conjugated donkey anti-rabbit, and IRDye 800

conjugated goat anti-mouse (Licor Inc.). Immunoblots were scanned with an Odyssey Imaging System (Licor Inc.).

Comet assay

To detect DNA damage we used comet assays following published protocols.[8, 9] Briefly, neonatal and adult c-kit$^+$ cells, c-kit$^+$ depleted non-cardiomyocytes and NIH 3T3 cells (ATCC) were plated overnight and incubated with 0.5μM DOX for 4 or 24 hrs, trypsinized and embedded in 1% low melt-point agarose and added to microscope slides at about 8000 cells/slide. The slides were subjected to alkaline lysis solution at 4˚C overnight, followed by gel electrophoresis. Slides were neutralized, stained with propidium iodide and imaged using an upright Zeiss Axiovision epifluorescent microscope. At least 50 nuclei were imaged and analyzed for each condition for every experiment. The aggregate result is a combination of 3 separate experiments. Data were analyzed using the OpenComet plugin for Image J.[10]

Flow cytometry

To determine the frequency of lineage-traced endothelial cells, we performed flow cytometry using a BD Facs Aria II (Becton, Dickenson and Company). Cells were isolated from adult hearts after saline or DOX treatment using Collagenase B, Dispase II digestion, combined with DNAse treatment. Following cell isolation, cells were stained with fluorophore-conjugated primary antibodies for CD31. Propidium iodide was used to select only live cells. GFP was readily detected without the need for antibody detection. FACS data were analyzed using FlowJo version 10.

RNA sequencing analysis

Single cell RNA-sequencing data processing and cell clustering

Raw single cell RNA sequencing data was plotted in a matrix consisting of 23425 genes and 405 cells. We removed genes that were expressed two cells or less, and removed cells that expressed fewer than 1000 genes. This filtering step resulted in a matrix consisting expression data of 13443 genes from 281 cells. We used the R / DEseq2 package to normalize the read count data and performed Principal Component Analysis(PCA).[11] We removed the first principal component, since this component was highly correlated with the number of expressed genes. We used t-SNE to visualize the data with 5% of the eigen components, as the use of 4% to 7% of eigen components showed higher accuracy in clustering of single cell RNA sequencing data.[12] We used R / Rtsne software with a default perplexity parameter of 30.[13] We clustered cells into four clusters using Partitioning Around Medoids (PAM) clustering algorithm. The number of cluster groups is determined based on gap statistic.[14] To further identify similarities between the cells within these four cell clusters, and known cardiac cell types, we used gene lists that identified fibroblast, endothelial and cardiomyocyte specific genes.[15-17] The expression level of genes is visualized on a heat map with respect to cell labels and cell clustering groups. We co-visualized our single cell RNA seq results with previously published bulk RNA sequencing samples to understand the likely identity of identified cell groups. We processed 20 bulk samples, 5 from fibroblasts[18], 3 from endothelial cells[19] and 12 from cardiomyocytes.[20-22] We combined these bulk RNA sequencing samples with our single cell RNA sequencing samples. To optimize co-visualization between bulk and single cell samples, we performed PCA and removed 4 PCs that had significant difference between bulk and single cell samples using Wilcoxon rank sum test. After this filtering, single cells and bulk samples were co-visualized using t-SNE.

Difference between CD45$^-$c-kit$^+$ cells harvested from different mouse models

To test the difference in gene expression of adult CD45$^-$c-kit$^+$ cells harvested from wild type or Kit$^{+/MCM}$ mice, we selected 293 genes previously identified to be

important in distinguishing cardiac c-kit^{+} cells from other progenitor cells.[23] We performed MAST, a statistical test for differential expression of single cell RNA sequencing data, to test whether these 293 genes are differentially expressed in c-kit targeted and wild type adult CD45^{-}c-kit^{+} cells.[24] Only one gene out of 293 genes, Mthfd1l, was statistically significant after FDR adjustment ($p<0.05$). We visualized gene expression data in a heat map plotting expression for all c-kit targeted and wild type adult CD45^{-}c-kit^{+} cells.

Bulk RNA sequencing after saline or DOX

Adult wild type mice were injected with saline or 10mg/kg DOX. Four days after injection we isolated CD45^{-}c-kit^{+} cells following the protocol described above. We pooled CD45^{-}c-kit^{+} cells from 3-5 mice into 3 saline, and 5 DOX treated experimental replicates (representing 12 saline and 20 DOX treated mice). RNA was isolated using the Norgen RNA purification kit according to the manufacturer's specifications. RNA quantification (Pico Green), library preparation and RNA sequencing was performed by the University of Minnesota Genomics Center. The library was size selected to produce insert sizes of ~200bp, and 50 bp pair-end run was performed on an Illumina HiSeq2500 for greater than 20 million reads for each library. The raw RNA-seq reads were mapped to the mouse genome (mm10) by TopHat (v2.0.13) and Cufflinks (v2.2.1) pipeline. Differential expression analysis was performed by DESeq; Fisher's exact test was used to determine significance. For qPCR, we injected 8 mice with saline and 8 mice with 10mg/kg DOX and isolated CD45^{-}c-kit^{+} cells. For qPCR we did not pool cells from different mice. We isolated RNA using the Norgen Single Cell RNA Purification kit, and quantified RNA using the Norgen Low Abundance RNA Quantification Kit according to the manufacturer's specifications. We normalized input RNA and generated cDNA using a Superscript VILO cDNA synthesis kit (Invitrogen). We ordered Taqman primers and probes and performed qPCR on a 7900HT Fast Real-Time PCR System (Applied

Biosystems). Relative Real-time PCR quantification was normalized to GAPDH based on the 2(-delta delta C(t)) method.[25]

Statistics

Results are described as mean ± SEM. Student's t-tests were performed when comparing 2 conditions, ANOVA followed by Tukey's HSD *post-hoc* analysis was used for multiple condition comparison. A p-value less than 0.05 was considered significant.

Supplemental Table 1. Overview of primary antibodies used.

Antigen	Manufacturer	Catalog #	Type	Immuno-histochemistry	Flow cytometry	Western blot
CD31	BD Bioscience	553370	Rat monoclonal	1:200		
CD45	R&D systems	AF114	Goat polyclonal	1:200		
Vimentin	Abcam	Ab45939	Rabbit polyclonal	1:200		
Troponin T	Cell signaling	5593	Rabbit polyclonal	1:250		
GATA4	R&D systems	AF2606	Goat polyclonal	1:200		
Kdr	R&D systems	AF644	Mouse polyclonal	1:50		
γH2Ax	Cell signaling	9718	Rabbit monoclonal	1:400		
P53	Santa Cruz	Sc-6243	Rabbit polyclonal	1:100		
53BP1	Novus Biologicals	NB100-304	Rabbit polyclonal	1:200		
CD31	eBioscience	Clone MEC13.3	Rat monoclonal		1:100	
CD45	BD Bioscience	Clone 104	Goat polyclonal		1:200	
P53	Cell Signaling Technology	2524	Rabbit polyclonal			1:1000
Cleaved Caspase 3	Cell Signaling Technology	9661	Rabbit polyclonal			1:1000
GAPDH	Fitzgerald Industries International	10R-G109a	Mouse monoclonal			1:1,000
Nkx2-5	Santa Cruz	sc-8697	Goat polyclonal	1:50		

Supplemental Table 2. Cardiac function measured by echocardiography in response to the indicated treatments. Presented are means of measured values. *p<0.05 vs echocardiographic measurement before treatment.

Genotype	Treatment	N	LVEDD (mm)	LVESD (mm)	FS (%)
R-GFP	DOX 2x10mg	10	3.78	2.74	28.0*
$Kit^{+/MCM}$ X R-GFP	DOX 2x10mg	10	3.78	2.82	26.6*
$Kit^{+/MCM}$ X R-GFP	DOX 1x10mg	4	3.86	2.24	42.1
$Kit^{+/MCM}$ X R-GFP	DOX 1x5mg	4	3.47	2.22	42.0

Supplemental Table 3. Overview of genes with significantly altered gene expression measured by RNA sequencing of CD45-c-kit+ cells harvested 4 days after saline or Doxorubicin (10mg/kg) injection, based on RNA seq of 3 and 5 pooled samples respectively.

Symbol	Gene name	Reference seq	Fold Change	P value
Rab3b	RAB3B, member RAS oncogene family	NM_023537	-6.40	3.58E-12
Nefl	neurofilament, light polypeptide	NM_010910	-6.38	2.07E-12
Gpr34	G protein-coupled receptor 34	NM_011823	-6.36	1.21E-12
Ntrk3	neurotrophic tyrosine kinase, receptor, type 3	NM_182809	-6.27	1.66E-10
Bnc1	basonuclin 1	NM_007562	-6.21	2.11E-11
Gpt	glutamic pyruvic transaminase, soluble	NM_182805	-5.62	1.94E-10
Th	tyrosine hydroxylase	NM_009377	-5.60	8.09E-09
Cib2	calcium and integrin binding family member 2	NM_019686	-5.60	8.34E-09
Lrrc48	leucine rich repeat containing 48	NM_029044	-5.54	8.34E-09
Echdc3	enoyl Coenzyme A hydratase domain containing 3	NM_024208	-5.53	4.25E-08
Zfp618	zinc finger protein 618	NM_028326	-5.48	3.84E-15
2900005J15Rik	RIKEN cDNA 2900005J15 gene	NR_027851	-5.47	6.15E-08
Abhd3	abhydrolase domain containing 3	NM_134130	-5.45	1.66E-10
Gm684	predicted gene 684	NM_001195681	-5.29	6.15E-08
Ebf4	early B cell factor 4	NM_001110513	-5.25	1.41E-07
Tyro3	TYRO3 protein tyrosine kinase 3	NM_019392	-5.14	3.27E-06
Ptprn	protein tyrosine phosphatase, receptor type, N	NM_008985	-5.12	9.22E-07
Rassf7	Ras association (RalGDS/AF-6) domain family (N-terminal) member 7	NM_025886	-5.09	1.04E-06
Cyp2d11	cytochrome P450, family 2, subfamily d, polypeptide 11	NM_001104531	-4.90	5.94E-07
AA986860	expressed sequence AA986860	NM_177604	-4.79	4.01E-05
Wfdc21	WAP four-disulfide core domain 21	NM_183249	-4.73	4.01E-05
Dancr	differentiation antagonizing non-protein coding RNA	NR_015531	-4.65	4.53E-05
Lacc1	laccase (multicopper oxidoreductase) domain containing 1	NM_172488	-4.59	6.72E-05
Exd1	exonuclease 3'-5' domain containing 1	NM_172857	-4.48	2.36E-04
Zscan20	zinc finger and SCAN domains 20	NM_177758	-4.40	1.43E-04
Cd79b	CD79B antigen	NM_008339	-4.39	4.20E-04

Adap1	ArfGAP with dual PH domains 1	NM_172723	-4.38	2.07E-04
4930563E22Rik	RIKEN cDNA 4930563E22 gene	NM_001163728	-4.33	5.38E-04
Skida1	SKI/DACH domain containing 1	NM_028317	-4.30	4.48E-04
Gm10451	predicted gene 10451	NR_028520	-4.29	3.75E-04
Wdr38	WD repeat domain 38	NM_029687	-4.24	8.36E-04
Pls1	plastin 1 (I-isoform)	NM_001033210	-4.20	1.45E-04
2010003K11Rik	RIKEN cDNA 2010003K11 gene	NM_027237	-4.20	1.01E-03
Zfp551	zinc fingr protein 551	NM_001033820	-4.17	1.29E-04
A230073K19Rik	RIKEN cDNA A230073K19 gene	NR_033229	-4.12	1.30E-03
Prkag2os1	protein kinase, AMP-activated, gamma 2 non-catalytic subunit, opposite strand 1	NR_040684	-4.11	1.61E-03
Gpsm2	G-protein signalling modulator 2 (AGS3-like, C. elegans)	NM_029522	-4.11	3.56E-04
Ckmt1	creatine kinase, mitochondrial 1, ubiquitous	NM_009897	-4.06	2.06E-04
Agfg2	ArfGAP with FG repeats 2	NM_145566	-4.04	1.58E-03
4632428C04Rik	RIKEN cDNA 4632428C04 gene	NR_033631	-4.02	1.61E-03
Lctl	lactase-like	NM_145835	-4.01	2.36E-03
Ccdc92	coiled-coil domain containing 92	NM_144819	-4.01	2.68E-03
Aldh1b1	aldehyde dehydrogenase 1 family, member B1	NM_028270	-3.97	2.49E-03
9430083A17Rik	RIKEN cDNA 9430083A17 gene	NR_029463	-3.95	3.27E-03
Rapgef6	Rap guanine nucleotide exchange factor (GEF) 6	NM_001252498	-3.93	3.50E-03
Tstd1	thiosulfate sulfurtransferase (rhodanese)-like domain containing 1	NM_001164525	-3.86	2.06E-04
A230020J21Rik	RIKEN cDNA A230020J21 gene	NR_027298	-3.85	3.34E-03
Actr3b	ARP3 actin-related protein 3B	NM_001004365	-3.82	4.95E-03
Slc5a6	solute carrier family 5 (sodium-dependent vitamin transporter), member 6	NM_001177622	-3.77	4.05E-03
Tmem26	transmembrane protein 26	NM_177794	-3.77	5.38E-04
Ttll6	tubulin tyrosine ligase-like family, member 6	NM_172799	-3.76	6.93E-03
Gm3604	predicted gene 3604	NM_001162910	-3.67	2.49E-08
Mkrn2os	makorin, ring finger protein 2, opposite strand	NM_001101431	-3.67	8.04E-03
Scml2	sex comb on midleg-like 2 (Drosophila)	NM_133194	-3.64	1.08E-02
Sgtb	small glutamine-rich tetratricopeptide repeat (TPR)-containing, beta	NM_144838	-3.62	1.01E-03
Slc9a9	solute carrier family 9 (sodium/hydrogen exchanger),	NM_177909	-3.62	2.49E-03

	member 9			
Gm20337	predicted gene, 20337	NR_045057	-3.59	5.76E-03
1700066B19Rik	RIKEN cDNA 1700066B19 gene	NM_001033168	-3.58	2.03E-03
Mks1	Meckel syndrome, type 1	NM_001039684	-3.58	3.03E-03
Tha1	threonine aldolase 1	NM_027919	-3.58	2.68E-03
Slc38a7	solute carrier family 38, member 7	NM_172758	-3.54	4.95E-03
Cd59a	CD59a antigen	NM_001111060	-3.53	2.02E-03
Nqo2	NAD(P)H dehydrogenase, quinone 2	NM_001163242	-3.51	1.61E-03
Acaa1b	acetyl-Coenzyme A acyltransferase 1B	NM_146230	-3.48	2.04E-02
Mfsd7c	major facilitator superfamily domain containing 7C	NM_145447	-3.46	1.93E-03
Chrm2	cholinergic receptor, muscarinic 2, cardiac	NM_203491	-3.43	2.48E-02
Irf4	interferon regulatory factor 4	NM_013674	-3.42	2.37E-02
Omp	olfactory marker protein	NM_011010	-3.41	2.54E-02
Zfp839	zinc finger protein 839	NM_028365	-3.39	2.35E-02
Adssl1	adenylosuccinate synthetase like 1	NM_007421	-3.39	1.14E-02
Grb7	growth factor receptor bound protein 7	NM_010346	-3.39	2.03E-02
Lrrc27	leucine rich repeat containing 27	NM_027164	-3.37	2.75E-02
Mir199a-1	microRNA 199a-1	NR_029585	-3.37	1.08E-02
Hp	haptoglobin	NM_017370	-3.36	2.32E-02
Zfp473	zinc finger protein 473	NM_178734	-3.36	1.08E-02
Twist2	twist basic helix-loop-helix transcription factor 2	NM_007855	-3.35	2.85E-02
Ggt7	gamma-glutamyltransferase 7	NM_144786	-3.35	3.12E-02
Myo5c	myosin VC	NM_001081322	-3.35	3.08E-02
Itih3	inter-alpha trypsin inhibitor, heavy chain 3	NM_008407	-3.34	4.95E-03
Hs3st3a1	heparan sulfate (glucosamine) 3-O-sulfotransferase 3A1	NM_178870	-3.32	3.37E-02
Hcar2	hydroxycarboxylic acid receptor 2	NM_030701	-3.32	3.01E-02
Sv2a	synaptic vesicle glycoprotein 2 a	NM_022030	-3.31	3.48E-02
Ifnlr1	interferon lambda receptor 1	NM_174851	-3.30	3.61E-02
Alx1	ALX homeobox 1	NM_172553	-3.29	3.58E-02
Nefm	neurofilament, medium polypeptide	NM_008691	-3.28	1.58E-02
Ngb	neuroglobin	NM_022414	-3.27	3.34E-02
Vat1l	vesicle amine transport protein 1 homolog-like (T. californica)	NM_173016	-3.26	3.95E-02
Ror2	receptor tyrosine kinase-like orphan receptor 2	NM_013846	-3.25	3.12E-02

Gm10516	predicted gene 10516	NR_033536	-3.24	4.07E-02
Atp6v1g2	ATPase, H+ transporting, lysosomal V1 subunit G2	NM_023179	-3.24	1.01E-02
Mal	myelin and lymphocyte protein, T cell differentiation protein	NM_010762	-3.23	6.93E-03
Wdr54	WD repeat domain 54	NM_023790	-3.23	4.25E-02
Lhfpl5	lipoma HMGIC fusion partner-like 5	NM_026571	-3.23	4.27E-02
Myot	myotilin	NM_001033621	-3.21	4.48E-02
Yeats2	YEATS domain containing 2	NM_001145931	-3.21	4.20E-02
Wnt5b	wingless-type MMTV integration site family, member 5B	NM_009525	-3.21	4.48E-02
Kctd19	potassium channel tetramerisation domain containing 19	NM_177791	-3.21	3.70E-02
Ly6g5b	lymphocyte antigen 6 complex, locus G5B	NM_148939	-3.20	5.76E-03
Cdhr1	cadherin-related family member 1	NM_130878	-3.20	4.48E-02
Clstn2	calsyntenin 2	NM_022319	-3.20	4.48E-02
Stac2	SH3 and cysteine rich domain 2	NM_146028	-3.18	3.03E-02
Rbfa	ribosome binding factor A	NM_199197	-3.17	8.22E-06
Zfp689	zinc finger protein 689	NM_175163	-3.16	1.61E-03
Tmem11	transmembrane protein 11	NM_001168507	-3.16	9.13E-03
Fam118a	family with sequence similarity 118, member A	NM_177067	-3.15	2.57E-02
Impa2	inositol (myo)-1(or 4)-monophosphatase 2	NM_053261	-3.14	2.03E-02
Spock2	sparc/osteonectin, cwcv and kazal-like domains proteoglycan 2	NM_052994	-3.12	2.02E-02
B630019K06Rik	novel protein similar to F-box and leucine-rich repeat protein 17 (Fbxl17)	NR_045448	-3.11	4.53E-02
Trnp1	TMF1-regulated nuclear protein 1	NM_001081156	-3.10	4.63E-02
Chrna3	cholinergic receptor, nicotinic, alpha polypeptide 3	NM_145129	-3.10	4.89E-02
Nppb	natriuretic peptide type B	NM_008726	-3.09	4.48E-02
Slc6a20b	solute carrier family 6 (neurotransmitter transporter), member 20B	NM_011731	-3.05	2.58E-02
Cdkn1a	cyclin-dependent kinase inhibitor 1A (P21)	NM_001111099	-3.05	4.12E-02
Rps19-ps3	ribosomal protein S19, pseudogene 3	NR_033639	-3.05	3.21E-03
Anks6	ankyrin repeat and sterile alpha motif domain containing 6	NM_001024136	-3.04	1.81E-02
Ropn1l	ropporin 1-like	NM_145852	-3.03	4.51E-02
Icam4	intercellular adhesion molecule 4, Landsteiner-Wiener blood group	NM_023892	-3.03	6.99E-03

Nol3	nucleolar protein 3 (apoptosis repressor with CARD domain)	NM_030152	-3.01	1.52E-02
9330159F19Rik	RIKEN cDNA 9330159F19 gene	NM_001162537	-3.00	2.45E-06
Mtbp	Mdm2, transformed 3T3 cell double minute p53 binding protein	NM_001168250	-2.99	2.46E-02
Cfd	complement factor D (adipsin)	NM_013459	-2.98	3.18E-02
Phospho1	phosphatase, orphan 1	NM_153104	-2.98	6.16E-03
Tigd3	tigger transposable element derived 3	NM_198634	-2.93	4.89E-03
Gnb3	guanine nucleotide binding protein (G protein), beta 3	NM_013530	-2.92	3.86E-02
Ppp1r16a	protein phosphatase 1, regulatory (inhibitor) subunit 16A	NM_033371	-2.91	9.38E-03
Panx1	pannexin 1	NM_019482	-2.86	1.07E-04
Wipf3	WAS/WASL interacting protein family, member 3	NM_001167860	-2.85	4.55E-02
Ngp	neutrophilic granule protein	NM_008694	-2.82	2.48E-02
Gtf2ird2	GTF2I repeat domain containing 2	NM_053266	-2.77	3.11E-02
Hpx	hemopexin	NM_017371	-2.76	2.37E-03
Cchcr1	coiled-coil alpha-helical rod protein 1	NM_146248	-2.76	9.94E-03
Rhot2	ras homolog gene family, member T2	NM_145999	-2.64	2.05E-03
1700096K18Rik	RIKEN cDNA 1700096K18 gene	NR_027388	-2.60	1.58E-03
Igdcc4	immunoglobulin superfamily, DCC subclass, member 4	NM_020043	-2.47	2.60E-02
Dlg2	discs, large homolog 2 (Drosophila)	NM_011807	-2.43	3.23E-02
Cyp2e1	cytochrome P450, family 2, subfamily e, polypeptide 1	NM_021282	-2.41	4.45E-02
Katnal1	katanin p60 subunit A-like 1	NM_153572	-2.36	1.49E-02
Tbc1d10a	TBC1 domain family, member 10a	NM_134023	-2.29	1.11E-02
Spa17	sperm autoantigenic protein 17	NM_011449	-2.12	2.03E-02
Syvn1	synovial apoptosis inhibitor 1, synoviolin	NM_028769	-2.09	3.39E-02
Slc10a7	solute carrier family 10 (sodium/bile acid cotransporter family), member 7	NM_029736	-1.94	3.90E-02
4930594C11Rik	G1 to S phase transition pseudogene	NR_024017	-1.83	7.88E-03
Nup133	nucleoporin 133	NM_172288	-1.71	2.75E-02
Malsu1	mitochondrial assembly of ribosomal large subunit 1	NM_029353	-1.62	1.72E-02
Aldh1a2	aldehyde dehydrogenase family 1, subfamily A2	NM_009022	-1.50	1.98E-02
Ccng1	cyclin G1	NM_009831	-1.41	4.48E-02
Tmem41b	transmembrane protein 41B	NM_153525	-1.38	3.34E-02

1110007C09Rik	RIKEN cDNA 1110007C09 gene	NM_026738	-1.35	3.36E-03
Mrpl39	mitochondrial ribosomal protein L39	NM_017404	-1.30	3.76E-02
Tstd3	thiosulfate sulfurtransferase (rhodanese)-like domain containing 3	NM_029840	-1.25	1.96E-02
Tm7sf3	transmembrane 7 superfamily member 3	NM_026281	-1.09	3.75E-02
Emc7	ER membrane protein complex subunit 7	NM_133749	-1.06	2.57E-03
Mgst1	microsomal glutathione S-transferase 1	NM_019946	-0.99	4.63E-02
Pgrmc2	progesterone receptor membrane component 2	NM_027558	-0.88	3.75E-02
Naa50	N(alpha)-acetyltransferase 50, NatE catalytic subunit	NM_028108	-0.87	4.89E-02
Pnkp	polynucleotide kinase 3'-phosphatase	NM_021549	-0.73	2.95E-02
Zscan26	zinc finger and SCAN domain containing 26	NM_001013786	-0.59	2.75E-02
Snx3	sorting nexin 3	NM_017472	-0.39	3.39E-02
Timp3	tissue inhibitor of metalloproteinase 3	NM_011595	0.22	2.23E-02
Fam198b	family with sequence similarity 198, member B	NM_133187	0.44	5.69E-03
Gosr2	golgi SNAP receptor complex member 2	NM_019650	0.47	3.65E-02
Rnf31	ring finger protein 31	NM_194346	0.55	2.48E-02
Grn	granulin	NM_008175	0.59	1.13E-02
Otud5	OTU domain containing 5	NM_138604	0.62	3.33E-02
Skiv2l2	superkiller viralicidic activity 2-like 2 (S. cerevisiae)	NM_028151	0.66	5.91E-03
Cdc40	cell division cycle 40	NM_027879	0.67	4.95E-03
Trmt10b	tRNA methyltransferase 10B	NM_027266	0.76	4.95E-03
Myh10	myosin, heavy polypeptide 10, non-muscle	NM_175260	0.82	4.27E-02
Plekhm1	pleckstrin homology domain containing, family M (with RUN domain) member 1	NM_183034	0.87	6.99E-03
Csnk1g1	casein kinase 1, gamma 1	NM_173185	0.87	9.77E-03
Ippk	inositol 1,3,4,5,6-pentakisphosphate 2-kinase	NM_199056	0.88	5.98E-03
Socs5	suppressor of cytokine signaling 5	NM_019654	0.92	5.76E-03
Gab1	growth factor receptor bound protein 2-associated protein 1	NM_021356	0.92	1.62E-02
Cog7	component of oligomeric golgi complex 7	NM_001033318	0.92	4.20E-02
Arhgef3	Rho guanine nucleotide exchange	NM_027871	0.93	3.37E-02

	factor (GEF) 3			
Slc41a1	solute carrier family 41, member 1	NM_173865	0.94	4.45E-02
Heyl	hairy/enhancer-of-split related with YRPW motif-like	NM_013905	0.95	2.32E-02
Zcchc24	zinc finger, CCHC domain containing 24	NM_001101433	0.95	5.91E-03
Apc	adenomatosis polyposis coli	NM_007462	0.97	4.15E-04
Tbcel	tubulin folding cofactor E-like	NM_173038	1.01	3.52E-04
Peak1	pseudopodium-enriched atypical kinase 1	NM_172924	1.03	1.01E-03
Cda	cytidine deaminase	NM_028176	1.07	3.90E-02
Cpm	carboxypeptidase M	NM_027468	1.14	1.13E-04
Sephs1	selenophosphate synthetase 1	NM_175400	1.16	1.81E-02
Aggf1	angiogenic factor with G patch and FHA domains 1	NM_025630	1.16	7.06E-03
Brf1	BRF1 homolog, subunit of RNA polymerase III transcription initiation factor IIIB (S. cerevisiae)	NM_028193	1.17	1.73E-03
Parg	poly (ADP-ribose) glycohydrolase	NM_011960	1.18	4.48E-02
Mef2a	myocyte enhancer factor 2A	NM_001033713	1.25	1.01E-02
Usp38	ubiquitin specific peptidase 38	NM_027554	1.25	1.15E-02
Tmem63a	transmembrane protein 63a	NM_144794	1.27	4.94E-02
Kdm5b	lysine (K)-specific demethylase 5B	NM_152895	1.37	2.64E-02
Csnk2a2	casein kinase 2, alpha prime polypeptide	NM_009974	1.38	6.07E-03
Pard3b	par-3 family cell polarity regulator beta	NM_001081050	1.39	2.84E-02
Adnp2	ADNP homeobox 2	NM_175028	1.41	3.26E-02
Cep72	centrosomal protein 72	NM_028959	1.48	6.99E-03
Cep290	centrosomal protein 290	NM_146009	1.51	3.31E-02
Slc41a2	solute carrier family 41, member 2	NM_177388	1.61	3.68E-02
Vhl	von Hippel-Lindau tumor suppressor	NM_009507	1.66	3.07E-02
Coq2	coenzyme Q2 homolog, prenyltransferase (yeast)	NM_027978	1.66	3.91E-02
Rptor	regulatory associated protein of MTOR, complex 1	NM_028898	1.67	2.03E-02
Coq10a	coenzyme Q10 homolog A (yeast)	NM_001081040	1.76	4.48E-02
Pbx3	pre B cell leukemia homeobox 3	NM_016768	1.78	4.89E-02
Bcdin3d	BCDIN3 domain containing	NM_029236	1.83	5.69E-04
Osbpl7	oxysterol binding protein-like 7	NM_001081434	1.83	2.03E-02
Zfp606	zinc finger protein 606	NM_026112	1.87	1.08E-02
Ago4	argonaute RISC catalytic subunit 4	NM_153177	2.01	4.27E-02
Plagl2	pleiomorphic adenoma gene-like 2	NM_018807	2.05	4.27E-04

Daam2	dishevelled associated activator of morphogenesis 2	NM_001008231	2.06	3.07E-02
Adamtsl1	ADAMTS-like 1	NM_029967	2.09	6.13E-03
Rad54l2	RAD54 like 2 (S. cerevisiae)	NM_030730	2.12	3.27E-03
Urb1	URB1 ribosome biogenesis 1 homolog (S. cerevisiae)	NM_029497	2.23	2.11E-02
Dzank1	double zinc ribbon and ankyrin repeat domains 1	NM_172859	2.36	9.95E-03
Pik3cb	phosphatidylinositol 3-kinase, catalytic, beta polypeptide	NM_029094	2.44	3.93E-03
Abca4	ATP-binding cassette, sub-family A (ABC1), member 4	NM_007378	2.72	4.27E-02
Macrod2	MACRO domain containing 2	NM_028387	2.91	2.97E-03
Ttc39c	tetratricopeptide repeat domain 39C	NM_028341	3.05	2.03E-02
4933417D19Rik	RIKEN cDNA 4933417D19 gene	NR_045849	3.06	3.75E-02
Snord15b	small nucleolar RNA, C/D box 14B	NR_002173	3.40	1.72E-02
Dpf3	D4, zinc and double PHD fingers, family 3	NM_058212	3.51	6.04E-04
Hal	histidine ammonia lyase	NM_010401	4.82	4.01E-05

Supplemental Table 4. Fold change in expression level of indicated genes in freshly isolated $CD45^{-}c\text{-}kit^{+}$ cells 4 days after Saline or Doxorubicin (10mg/kg) injection. N=8 for each group. * difference determined by Wilcoxon rank test.

Gene name	Saline	Doxorubicin	P value
Cdh5	1 ± 0.186	1.068 ± 0.056	0.736
Vim	1 ± 0.160	1.084 ± 0.113	0.676
Trp53	1 ± 0.144	1.152 ± 0.099	0.398
Gata4	1 ± 0.116	1.410 ± 0.179	0.075
Nkx2-5	1 ± 0.322	2.704 ± 0.357	**0.003**
Tbx5	1 ± 0.148	1.391 ± 0.204	0.143
Myh6	1 ± 0.219	2.638 ± 0.419	**0.004**
Myh7	1 ± 0.860	16.790 ± 7.607	**0.003***
Nppa	1 ± 0.247	2.710 ± 0.406	**0.003**
Nppb	1 ± 0.324	3.417 ± 0.557	**0.002**
Myot	1 ± 0.736	6.144 ± 2.375	0.071
Cib2	1 ± 0.427	2.899 ± 0.593	**0.021**

Supplemental Figure 1

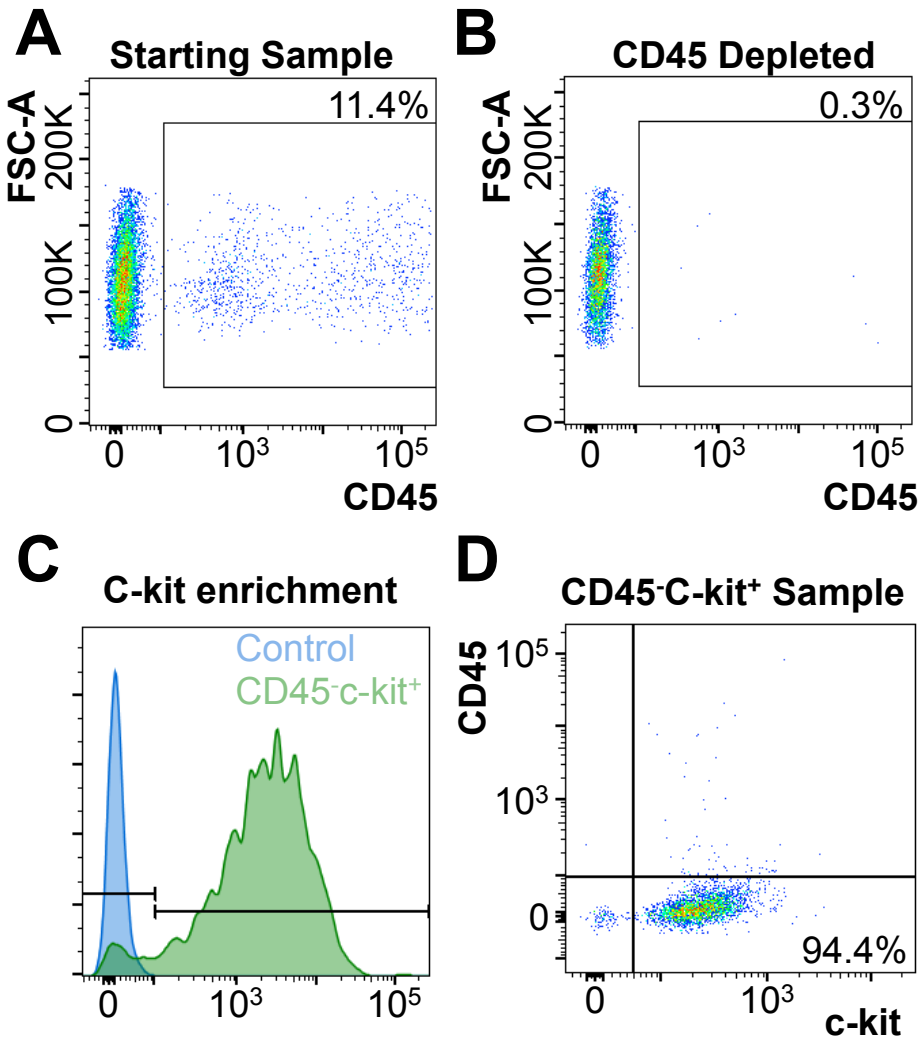

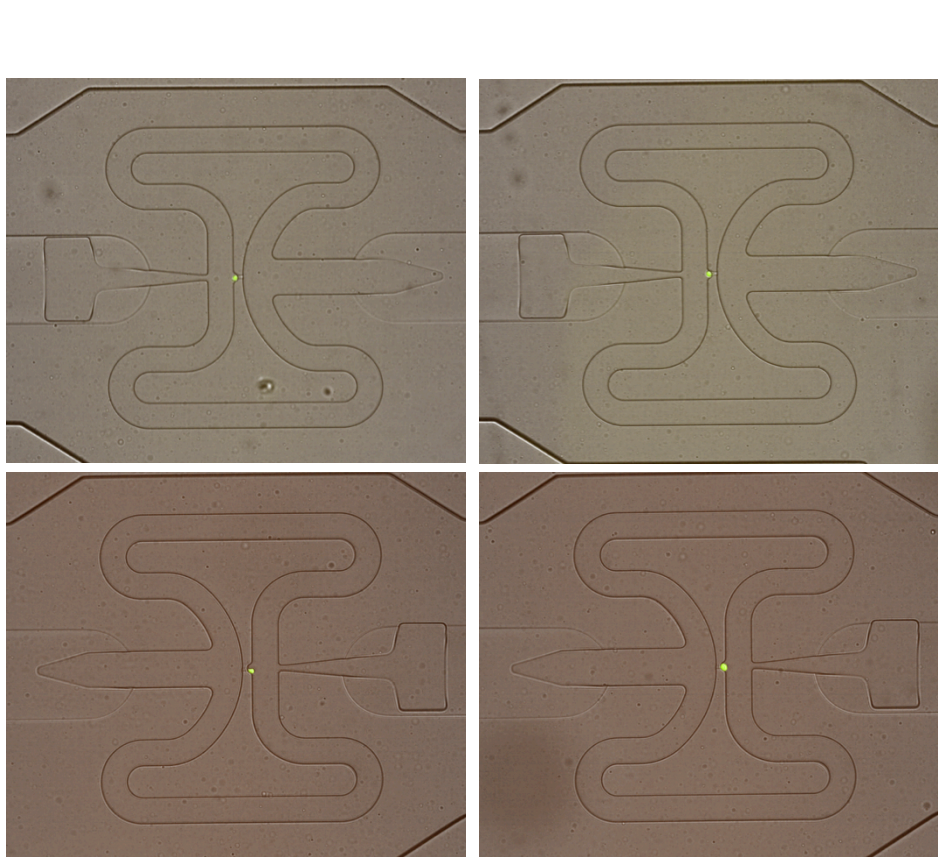

Supplemental Figure 2

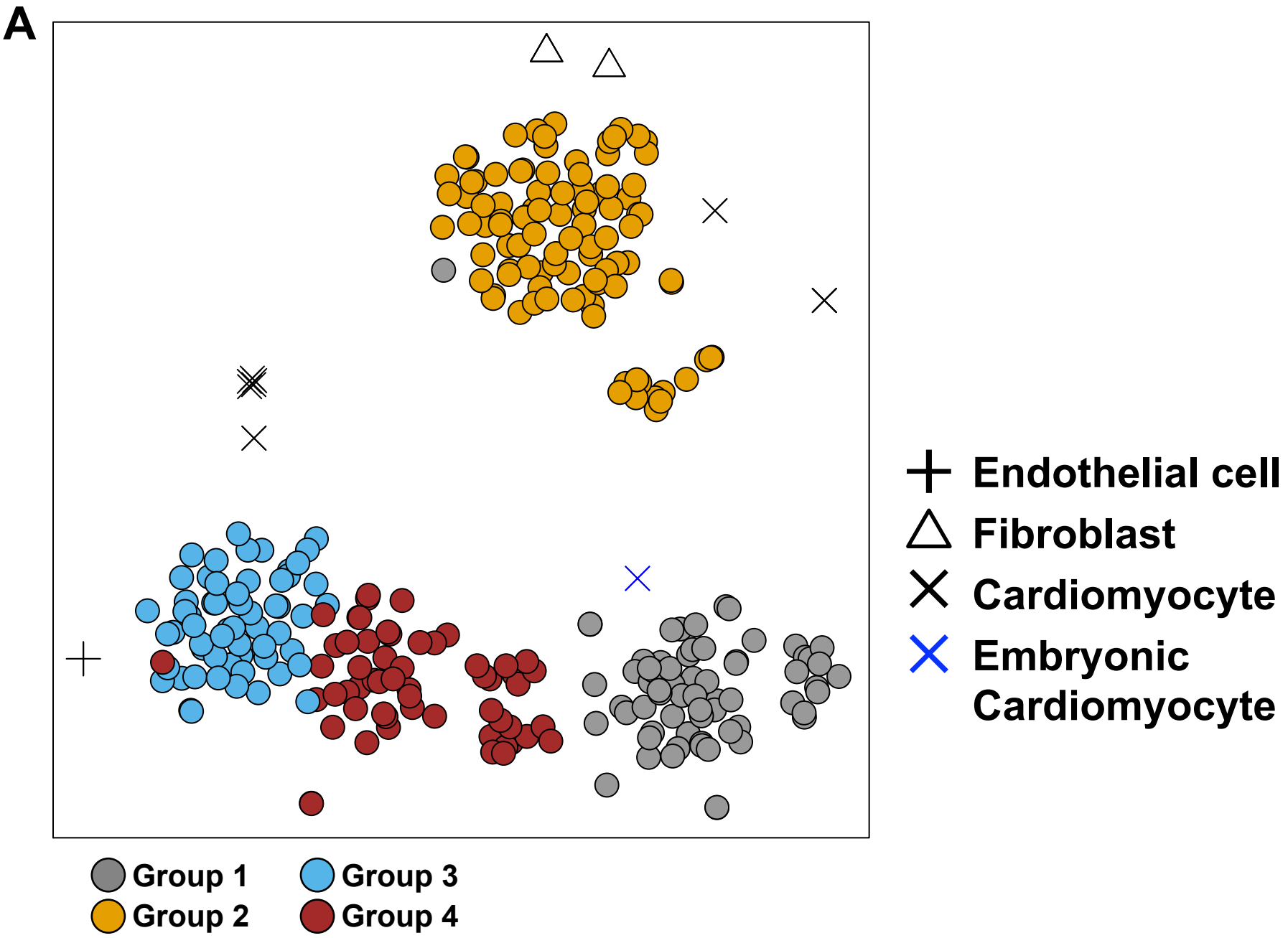

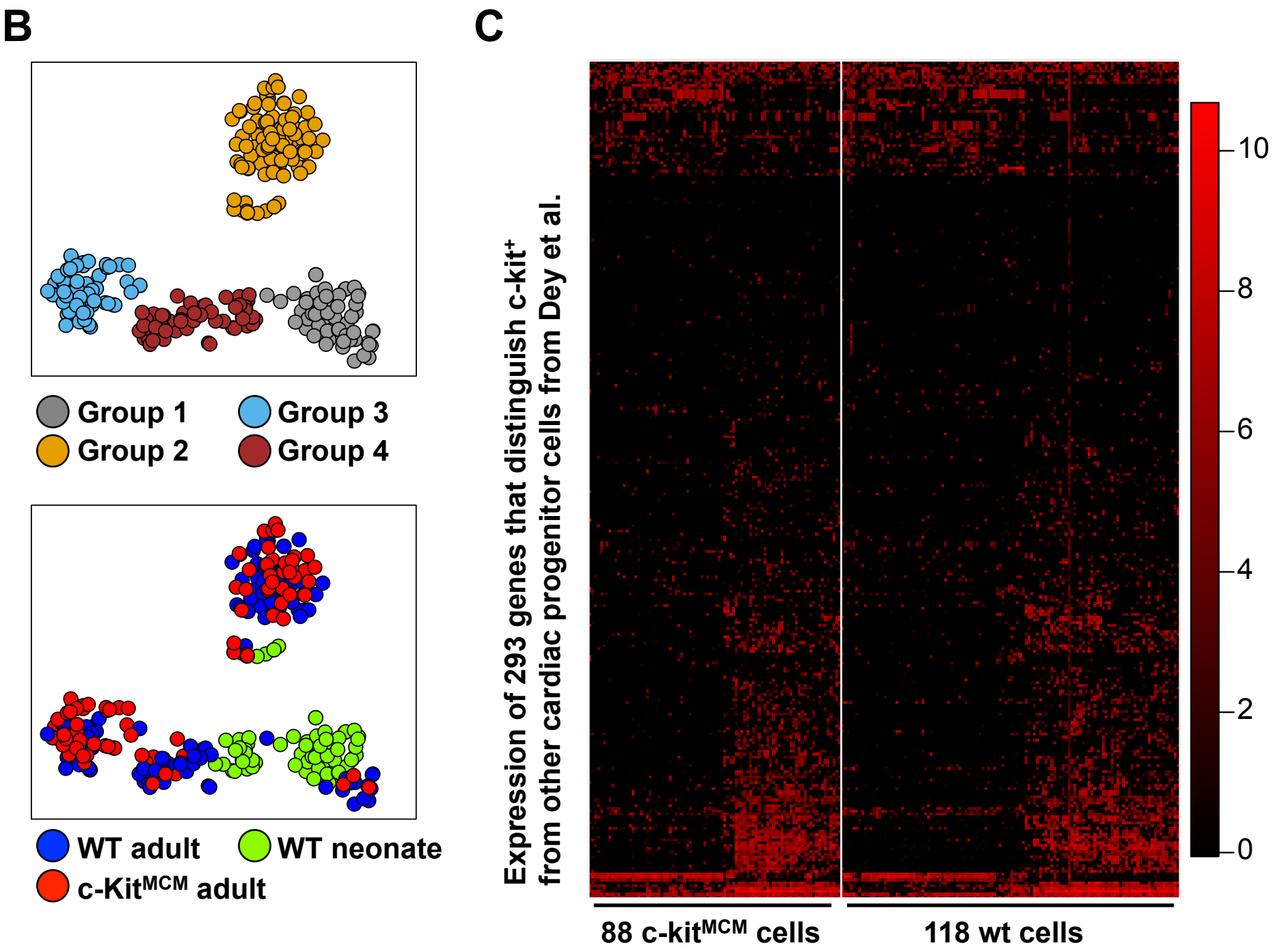
B
Group 1
Group 3
Group 2
Group 4
WT adult
WT neonate
c-Kit^MCM adult
C
Expression of 293 genes that distinguish c-kit+ from other cardiac progenitor cells from Dey et al.
88 c-kit^MCM cells
118 wt cells
10
8
6
4
2
0

Supplemental Figure 3

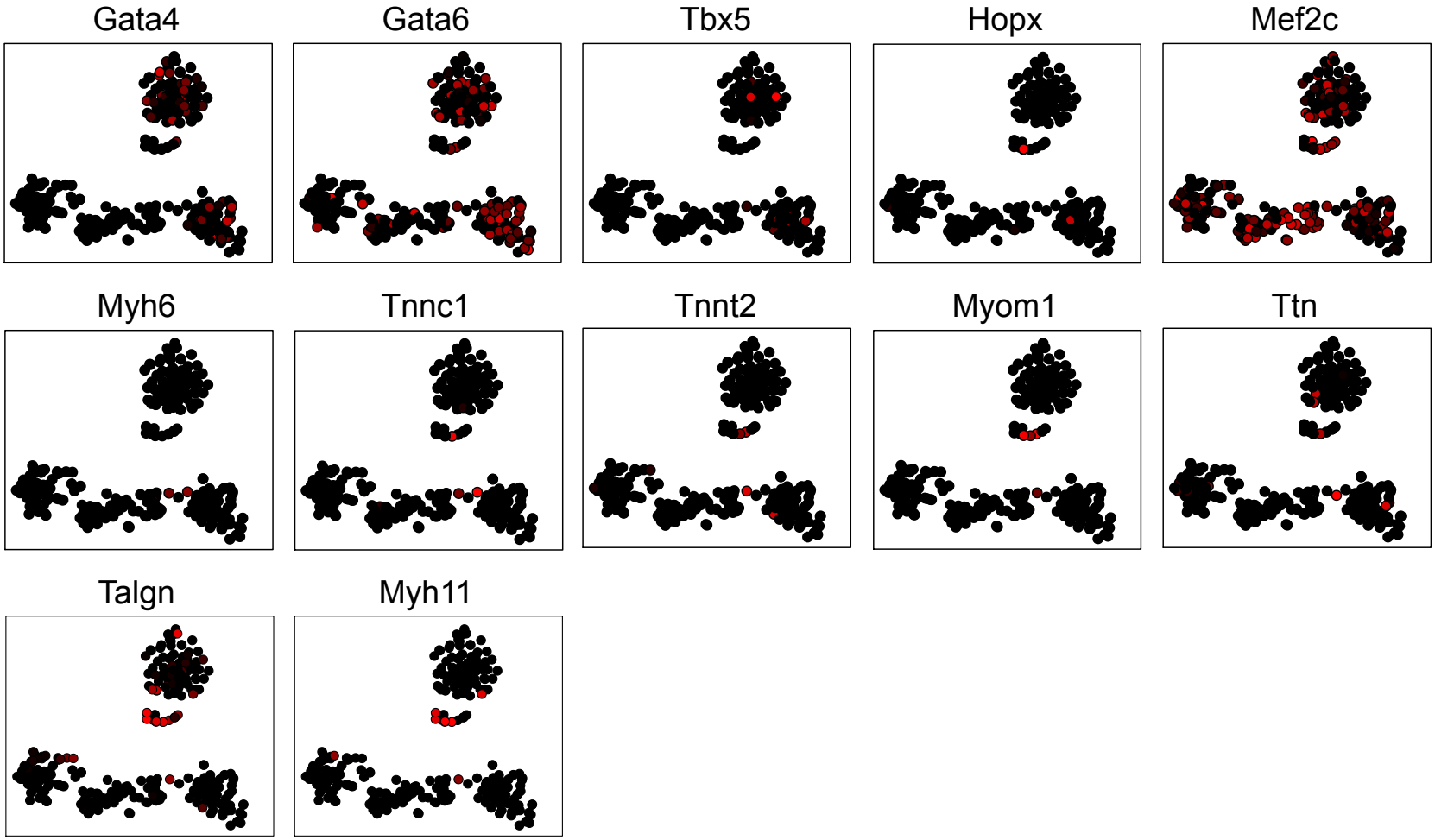

Supplemental Figure 4

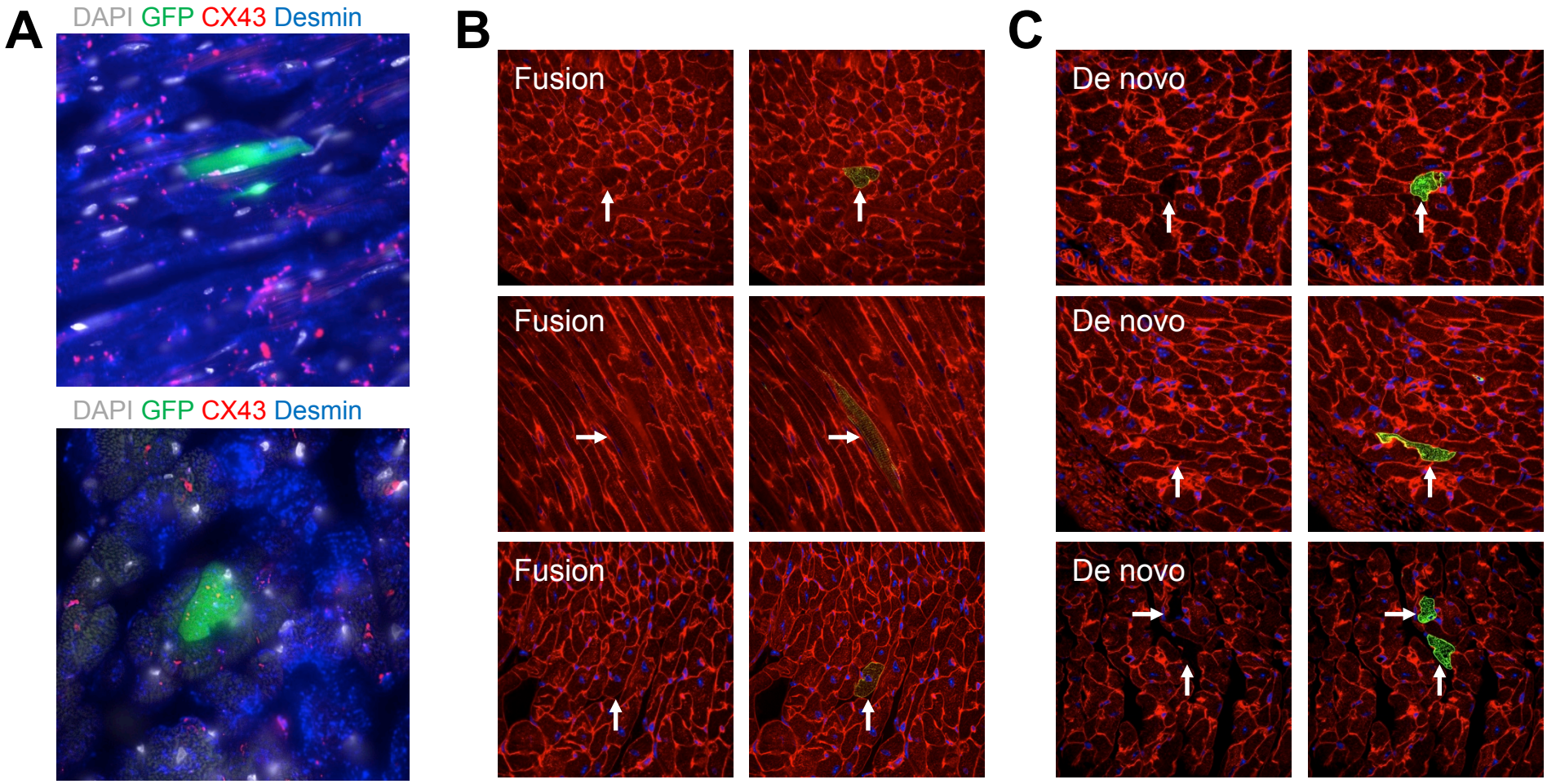

Supplemental Figure 5

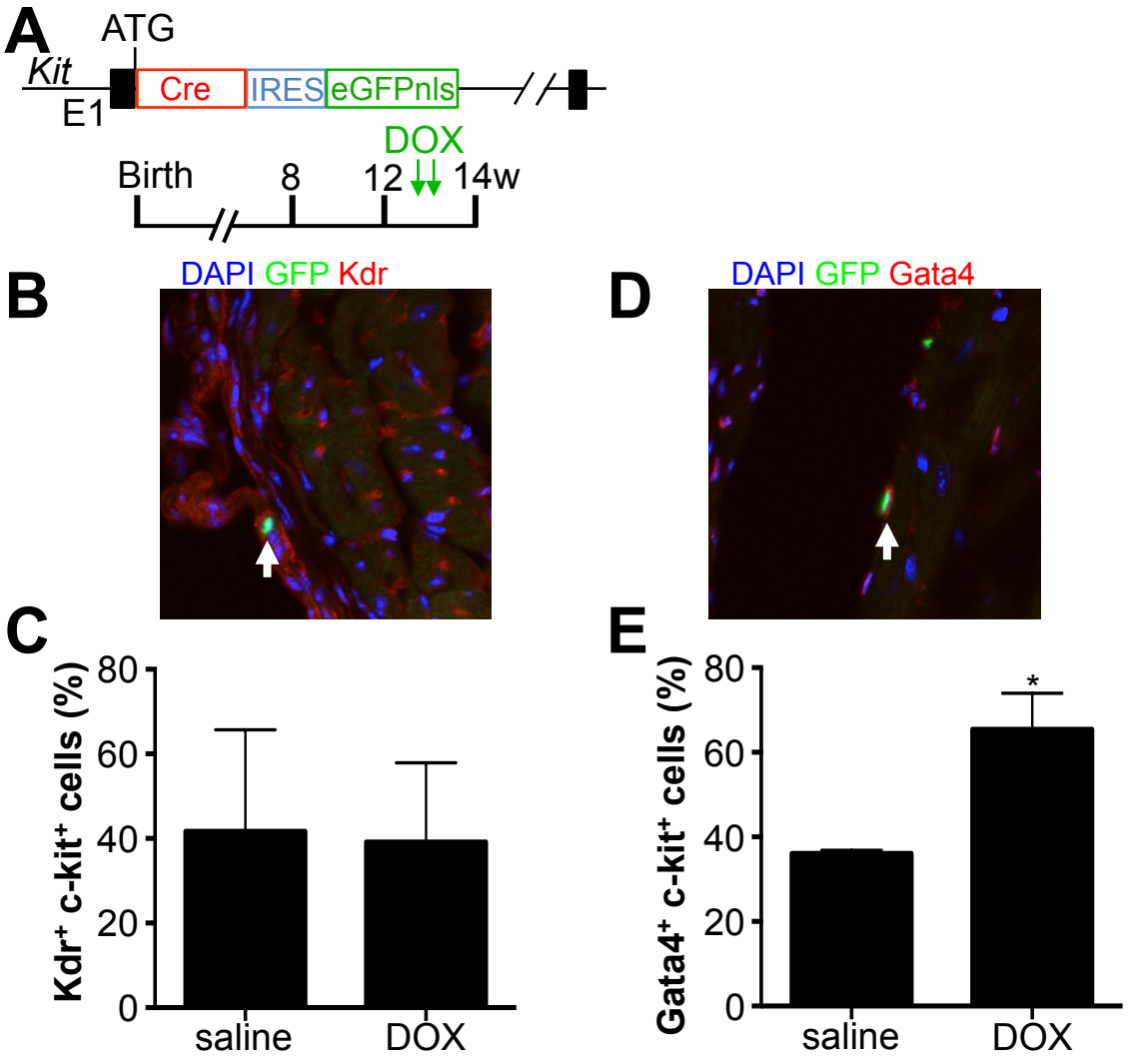

Supplemental Figure 6

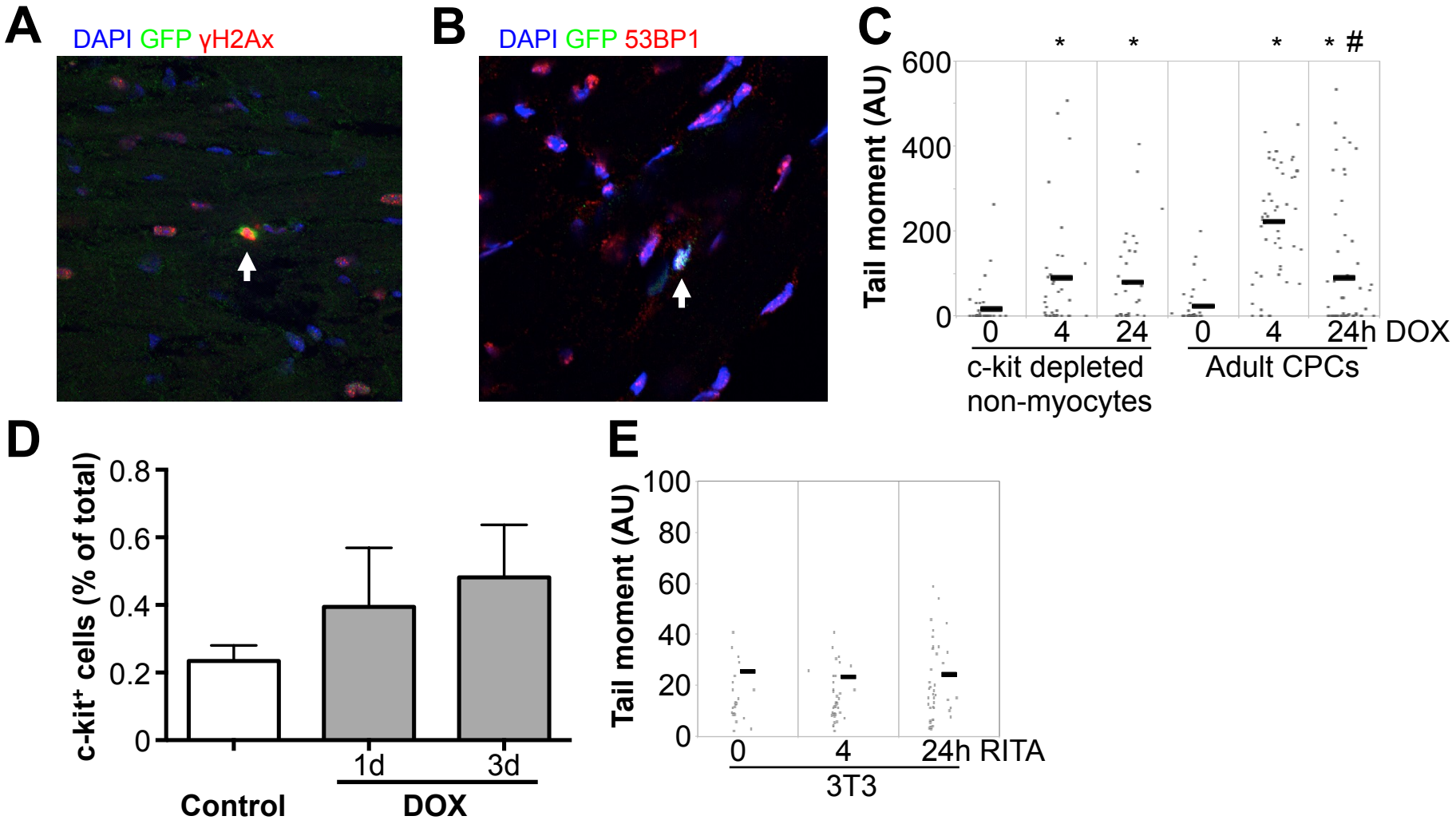

Supplemental Figure Legends

Supplemental Figure 1. Evaluation of the purity of isolated $CD45^{-}c\text{-}kit^{+}$ cells. Cells isolated from mice were stained with antibodies for CD45 (**A-D**) and c-kit (**C-D**), followed by flow cytometry assays. (**A, B**) CD45 expression in all non-cardiomyocytes isolated from the heart (**A**) and $CD45^{+}$-depleted cells (**B**); (**C**) $c\text{-}kit^{+}$ enrichment after positive selection with a magnetic bead conjugated c-kit-antibody; (**D**) CD45 and c-kit expression in a final cell sample. **E.** Examples of individual live single cells captured on Fluidigm small cell IFC (Green/Red is Live/Dead stain).

Supplemental Figure 2. Single Cell Sequencing of cardiac $CD45^{-}c\text{-}kit^{+}$ cells. **A.** Co-clustering between single cell sequenced CD45-c-kit+ cells and previously published RNA-seq datasets for endothelial cells, fibroblasts and cardiomyocytes, visualized on a t-SNE plot. **B.** Visualization of origin of cells used for single cell sequencing for identified clusters. **C.** Heatmap of genes selected from Dey et al. (PMID 23463815) as genes that distinguish cardiac-derived $c\text{-}kit^{+}$ cells from other progenitor cells. Plotted is a heatmap for all cells from adult wt and adult $Kit^{+/MCM}$ mice, which shows essentially no differences between wt and $Kit^{+/MCM}$ $c\text{-}kit^{+}$ cells.

Supplemental Figure 3. Heatmap expression of selected genes that are commonly expressed in cardiomyocytes (Gata4, Gata6, Tbx5, Hopx, Mef2c, Myh6, Tnnc1, Tnnt2, Myom1, Ttn) or smooth muscle cells (Talgn, Myh11) plotted onto single cell sequencing clusters failed to identify specific cells that are likely to become cardiomyocytes.

Supplemental Figure 4. A. Immunohistochemistry for DAPI (grey), GFP (green), Connexin 43 (red), Desmin (blue) showing normal Connexin 43 distribution in GFP^{+} cardiomyocytes. **(B-C)** Examples of Fusion and De Novo c-kit derived cardiomyocytes. **B.** Examples of Tomato and GFP double positive cardiomyocytes in response to DOX. **C.** Examples of GFP only positive cardiomyocytes in response to DOX

Supplemental Figure 5. A. Experimental design used in panels **B-E. B.** Immunohistochemistry for Kdr (red), GFP (green), DAPI (blue) showing Kdr expression in $c\text{-}kit^{+}$ cells. **C.** Quantification of Kdr expressing $c\text{-}kit^{+}$ cells. N=3 and 4 **D.** Representative immunohistochemistry for GATA4 (red), GFP (green), DAPI (blue) showing GATA4 expression in $c\text{-}kit^{+}$ cells. **E.** Quantification of GATA4 expressing $c\text{-}kit^{+}$ cells. N=3 and 4, *$p<0.05$

Supplemental Figure 6. A. Immunohistochemistry for γH2Ax (red), GFP (green), DAPI (blue) showing γH2Ax expression in $c\text{-}kit^{+}$ cells (green). **B.** Immunohistochemistry for 53BP1 (red), GFP (green), DAPI (blue) showing 53BP1 expression in $c\text{-}kit^{+}$ cells (green). **C.** $c\text{-}kit^{+}$ depleted non-myocytes and $c\text{-}kit^{+}$ CPCs isolated from adult mice were treated with 0.5μM DOX for 0, 4 or 24 hours, followed by comet assays. Depicted is the tail moment (indicative for DNA damage) at indicated time points after DOX addition **D.** Quantification of percentage of cells that stained positive for c-kit in saline or DOX treated hearts. **E.** Cultured 3T3fibroblasts were treated with 13nM RITA for 0, 4, or 24 hours. Tail moment was measured from individual cell images after comet assays. * $p<0.05$, compared with 0-hr c-kit depleted non-myocytes; # $p<0.05$, compared with 4-hr adult CPCs

Supplemental References

1. van Berlo JH, Kanisicak O, Maillet M, Vagnozzi RJ, Karch J, Lin SC, Middleton RC, Marbán E and Molkentin JD. c-kit+ cells minimally contribute cardiomyocytes to the heart. *Nature*. 2014;509:337-41.
2. García-Cao I, García-Cao M, Martín-Caballero J, Criado LM, Klatt P, Flores JM, Weill JC, Blasco MA and Serrano M. "Super p53" mice exhibit enhanced DNA damage response, are tumor resistant and age normally. *EMBO J*. 2002;21:6225-35.
3. Robinson SP, Langan-Fahey SM, Johnson DA and Jordan VC. Metabolites, pharmacodynamics, and pharmacokinetics of tamoxifen in rats and mice compared to the breast cancer patient. *Drug Metab Dispos*. 1991;19:36-43.
4. van Berlo JH, Elrod JW, van den Hoogenhof MM, York AJ, Aronow BJ, Duncan SA and Molkentin JD. The transcription factor GATA-6 regulates pathological cardiac hypertrophy. *Circ Res*. 2010;107:1032-40.
5. Smith AJ, Lewis FC, Aquila I, Waring CD, Nocera A, Agosti V, Nadal-Ginard B, Torella D and Ellison GM. Isolation and characterization of resident endogenous c-Kit+ cardiac stem cells from the adult mouse and rat heart. *Nat Protoc*. 2014;9:1662-81.
6. Gong W, Rasmussen TL, Singh BN, Koyano-Nakagawa N, Pan W and Garry DJ. Dpath software reveals hierarchical haemato-endothelial lineages of Etv2 progenitors based on single-cell transcriptome analysis. *Nat Commun*. 2017;8:14362.
7. Tallini YN, Greene KS, Craven M, Spealman A, Breitbach M, Smith J, Fisher PJ, Steffey M, Hesse M, Doran RM, Woods A, Singh B, Yen A, Fleischmann BK and Kotlikoff MI. c-kit expression identifies cardiovascular precursors in the neonatal heart. *Proc Natl Acad Sci U S A*. 2009;106:1808-13.
8. L'Ecuyer T, Sanjeev S, Thomas R, Novak R, Das L, Campbell W and Heide RV. DNA damage is an early event in doxorubicin-induced cardiac myocyte death. *Am J Physiol Heart Circ Physiol*. 2006;291:H1273-80.
9. Olive PL and Banáth JP. The comet assay: a method to measure DNA damage in individual cells. *Nat Protoc*. 2006;1:23-9.
10. Gyori BM, Venkatachalam G, Thiagarajan PS, Hsu D and Clement MV. OpenComet: an automated tool for comet assay image analysis. *Redox Biol*. 2014;2:457-65.
11. Love MI, Huber W and Anders S. Moderated estimation of fold change and dispersion for RNA-seq data with DESeq2. *Genome Biol*. 2014;15:550.
12. Kiselev VY, Kirschner K, Schaub MT, Andrews T, Yiu A, Chandra T, Natarajan KN, Reik W, Barahona M, Green AR and Hemberg M. SC3: consensus clustering of single-cell RNA-seq data. *Nat Methods*. 2017;14:483-486.
13. van der Maaten L and Hinton G. Visualizing Data using t-SNE. *Journal of Machine Learning Research*. 2008;9:2579-2605.
14. Tibshirani R, Walther G and Hastie T. Estimating the number of clusters in a data set via the gap statistic. *Journal of the Royal Statistical Society Series B (Statistical Methodology)*. 2001;63:411-423.
15. Li G, Plonowska K, Kuppusamy R, Sturzu A and Wu SM. Identification of cardiovascular lineage descendants at single-cell resolution. *Development*. 2015;142:846-57.
16. Li G, Xu A, Sim S, Priest JR, Tian X, Khan T, Quertermous T, Zhou B, Tsao PS, Quake SR and Wu SM. Transcriptomic Profiling Maps Anatomically Patterned Subpopulations among Single Embryonic Cardiac Cells. *Dev Cell*. 2016;39:491-507.
17. DeLaughter DM, Bick AG, Wakimoto H, McKean D, Gorham JM, Kathiriya IS, Hinson JT, Homsy J, Gray J, Pu W, Bruneau BG, Seidman JG and Seidman CE. Single-Cell Resolution of Temporal Gene Expression during Heart Development. *Dev Cell*. 2016;39:480-490.

18. Pillai IC, Li S, Romay M, Lam L, Lu Y, Huang J, Dillard N, Zemanova M, Rubbi L, Wang Y, Lee J, Xia M, Liang O, Xie YH, Pellegrini M, Lusis AJ and Deb A. Cardiac Fibroblasts Adopt Osteogenic Fates and Can Be Targeted to Attenuate Pathological Heart Calcification. *Cell Stem Cell*. 2017;20:218-232.e5.
19. Sangwung P, Zhou G, Nayak L, Chan ER, Kumar S, Kang DW, Zhang R, Liao X, Lu Y, Sugi K, Fujioka H, Shi H, Lapping SD, Ghosh CC, Higgins SJ, Parikh SM, Jo H and Jain MK. KLF2 and KLF4 control endothelial identity and vascular integrity. *JCI Insight*. 2017;2:e91700.
20. Greco CM, Kunderfranco P, Rubino M, Larcher V, Carullo P, Anselmo A, Kurz K, Carell T, Angius A, Latronico MV, Papait R and Condorelli G. DNA hydroxymethylation controls cardiomyocyte gene expression in development and hypertrophy. *Nat Commun*. 2016;7:12418.
21. Zhou H, Dickson ME, Kim MS, Bassel-Duby R and Olson EN. Akt1/protein kinase B enhances transcriptional reprogramming of fibroblasts to functional cardiomyocytes. *Proc Natl Acad Sci U S A*. 2015;112:11864-9.
22. Sprenger JU, Perera RK, Steinbrecher JH, Lehnart SE, Maier LS, Hasenfuss G and Nikolaev VO. In vivo model with targeted cAMP biosensor reveals changes in receptor-microdomain communication in cardiac disease. *Nat Commun*. 2015;6:6965.
23. Dey D, Han L, Bauer M, Sanada F, Oikonomopoulos A, Hosoda T, Unno K, De Almeida P, Leri A and Wu JC. Dissecting the molecular relationship among various cardiogenic progenitor cells. *Circ Res*. 2013;112:1253-62.
24. Finak G, McDavid A, Yajima M, Deng J, Gersuk V, Shalek AK, Slichter CK, Miller HW, McElrath MJ, Prlic M, Linsley PS and Gottardo R. MAST: a flexible statistical framework for assessing transcriptional changes and characterizing heterogeneity in single-cell RNA sequencing data. *Genome Biol*. 2015;16:278.
25. Livak KJ and Schmittgen TD. Analysis of relative gene expression data using real-time quantitative PCR and the 2(-Delta Delta C(T)) Method. *Methods*. 2001;25:402-8.